

Soil Loss Risk Analysis for Construction Activities

Billur Kazaz¹ , Jaime C. Schussler¹ ,
LouLou C. Dickey² , and Michael A. Perez¹ 

Transportation Research Record
2022, Vol. 2676(6) 503–513
© National Academy of Sciences:
Transportation Research Board 2022
Article reuse guidelines:
sagepub.com/journals-permissions
DOI: [10.1177/03611981221075027](https://doi.org/10.1177/03611981221075027)
journals.sagepub.com/home/trr



Abstract

Construction-related ground-disturbing activities leave exposed land susceptible to soil loss and increase the risk of polluting adjacent waterbodies with sediment-laden discharge. State and federal regulations require stormwater pollution prevention plans to be implemented during construction to mitigate the impact of stormwater runoff. Areas prone to soil loss can be identified early in site planning using soil loss modeling. Identification of these critical areas could influence the design and placement of erosion and sediment control practices. The Revised Universal Soil Loss Equation (RUSLE) can be applied to estimate the soil loss on construction sites in tonnes per Ha per year (tons/acre/year) by considering factors of rainfall erosivity, soil erodibility, length of slope, erosion control, and sediment control. This study integrates geographic information system (GIS) with RUSLE to create soil loss models for residential, commercial, and highway construction scenarios in the contiguous U.S.A. These three construction types were modeled in various locations throughout the country to assess erosive risk. Soil loss outputs were categorized into five risk tiers ranging from very low to very high. Southeastern states had the highest estimated soil loss during residential, commercial, and highway construction, reaching rates of 1,464, 706, and 1,302 tonnes per Ha per year (653, 315, and 581 tons/acre/year), respectively. This study provides a customizable model for any site-specific slope-length factor outside of the three construction scenarios modeled. Integration of GIS provides a unique opportunity to apply RUSLE across a larger landscape. The presented macro-scale data can be used for the design of erosion and sediment control practices.

Keywords

infrastructure, roadway design, hydrology and hydraulics and stormwater, stormwater management

Earthmoving operations during construction leave land exposed to wind and rainfall, increasing the risk of on-site erosion and off-site sediment deposition. In the U.S.A. construction sites disturbing areas larger than 0.4 Ha (1.0 acre) of land are required to follow National Pollutant Discharge Elimination System regulations which require construction operators to obtain a Construction General Permit (CGP) (1). The CGP emphasizes the significance of a well-developed Stormwater Pollution Prevention Plan (SWPPP) to limit environmental hazards implicated by stormwater runoff from construction activities (2). SWPPP documents include project information, erosion and sediment control (E&SC) plans, and a description of stormwater management practices planned for the site (3). Failure to comply with these requirements may result in regulatory actions such as fines or stop-work orders.

When properly designed and installed, E&SC practices protect downstream waterbodies by reducing erosion and capturing eroded sediment. Erosion control practices minimize the risk of dislodging soil by covering exposed land or slowing the overland flow of runoff. Proper placement of erosion control practices such as surface roughening, seeding, mulching, erosion control blankets, and slope drains can significantly minimize soil loss on construction sites (4). Conversely, sediment control practices capture dislodged sediment and reduce off-

¹Department of Civil and Environmental Engineering, Auburn University, Auburn, AL

²Department of Civil, Construction and Environmental Engineering, Iowa State University, Ames, IA

Corresponding Author:
Billur Kazaz, bzk0061@auburn.edu

site transport of soil. Sediment control practices include sediment barriers, inlet protection, and sedimentation basins, amongst others (4–6). The success of an E&SC plan, and in turn a site's SWPPP, is dependent on the appropriate design, installation, and maintenance practices used on site. Calculating soil loss can serve as an essential component to develop SWPPPs; however, soil loss models are rarely used in planning phases. Soil loss models rely on input variables including rainfall data, soil characteristics, topography, cover practices, and sediment management practices to identify critical areas on site that are susceptible to severe erosion (7). Model outputs provide estimates of soil loss and thus inform designers of critical site areas that require meticulous care and detail when planning E&SC practices (8).

Construction sites are highly dynamic with phasing, changing topography, non-uniform soil distributions, varying cover conditions, and seasonal precipitation. These factors make it challenging to apply a soil loss model that produces an accurate, consistent representation of site conditions. The Revised Universal Soil Loss Equation (RUSLE) is a robust soil loss model that estimates soil loss in tonnes per Ha per year (tons/acre/year). RUSLE models are limited to analyzing individual slopes and thus are not commonly used by stormwater professionals for soil loss estimation during the development of SWPPPs. RUSLE is often used as a forensic tool during disputes and litigation to determine the quantity of soil that must be mitigated or removed from downstream areas. However, a ready-to-use soil loss model could aid designers in SWPPP development and provide rapid identification of areas at risk that require E&SC practices.

The aim of this study was to provide a soil loss tool for designers to compare critical areas and SWPPP designs by integrating geographic information system (GIS) mapping with RUSLE. Amounts of soil loss were calculated by using RUSLE principles and the data were visualized for the purpose of providing a user-friendly soil loss risk assessment model. As a result, a soil loss model was developed for the contiguous United States (CONUS) by computing each RUSLE parameter on a national scale. An additional model excluding the slope-length factor was developed to allow designers to input this parameter for site-specific slope-length conditions. The study calculated slope-length parameters on representative construction site plans and considered three different construction scenarios: (i) residential, (ii) commercial, and (iii) highway. Amounts of soil loss from these construction scenarios were visualized and analyzed to make the soil loss model adaptable for any potential construction site in CONUS. Furthermore, the results identified critical locations at risk for high soil loss rates across the residential, commercial, and highway construction site cases.

Literature Review

The Dust Bowl of the 1930s was a pivotal contributor toward the development of soil conservation efforts in the U.S.A. Soil loss estimation, originally developed for agricultural applications, has progressed from early techniques as computer-based soil models have been developed (7, 9). The use of these models has also evolved to applications outside of agriculture to the construction, forestry, and mining sectors (10–12). The Universal Soil Loss Equation (USLE), Modified Universal Soil Loss Equation (MUSLE), and RUSLE are the most commonly used soil loss models. USLE and RUSLE use rainfall erosivity, whereas MUSLE relies on runoff volume and peak flow rate (13–15). RUSLE simulates soil loss by using process-based supporting parameters, and MUSLE predicts sediment yield by simulating individual storms (16).

USLE is an empirical approach capable of estimating long-term soil loss for sheet and interrill erosion (13). The model considers rainfall, soil, topography, vegetation, and support practices and multiplies these factors to calculate soil loss in mass/unit area/year (13), using the equation presented in Equation 1.

$$A = R * K * LS * C * P \quad \text{δ1P}$$

where

A = soil loss, in tonnes/Ha/year (tons/acre/year)

R = rainfall erosivity factor, in hundreds of meter tonnes $\text{Ha}^{21} \text{ year}^{21}$ in h^{21} (hundreds of ft tons acre 21 year 21 in h 21)

K = soil erodibility factor, in tonnes/Ha (hundreds of meter tonnes Ha^{21} in h^{21}) 21 (tons acre 21 (hundreds of ft tons acre 21 in h 21) 21)

LS = slope-length factor

C = cover management factor

P = support practice factor.

USLE was developed based on the unit plot conditions of 22.1 m (72.6 ft) slope length and 9% slope and mainly focused on small areas or uniform hillslopes, which resulted in limited soil loss estimation results (9). With its reliance on paper-based tables and charts, USLE has become outdated. According to an error assessment study by Risse et al. (17), USLE provided accurate results for average annual soil loss but not for annual soil loss. Thus, the need for revision and modification of USLE emerged, which prompted the development of RUSLE.

RUSLE, a revised version of USLE, depends on the same input parameters as USLE, but with improvements (14, 18). RUSLE automated soil loss estimation procedures by calculating amounts of soil loss using computer-based software (9). In late 1992, the development of RUSLE enhanced the accuracy of the USLE parameters by deriving rainfall erosivity from a database for the

U.S.A., developing a time-varying soil erodibility factor suitable for freezing and thawing conditions, providing new algorithms for topographic factors considering rill versus interrill erosion ratio, changing the cover management factor to a continuous function, and improving the support practice factor database with additional practices (14). RUSLE2 is a computer database version that was released in 2004. RUSLE2 has further improved database features that implement the same principles as RUSLE but relies on software to simplify parameter selection and calculate the soil loss model. Similarly, RUSLE2 is limited to analysis on an individual slope (9).

The computerization of USLE/RUSLE provided opportunities to integrate innovative technologies with soil loss modeling; GIS is one application of this technology. GIS is a computer-based system representing geographical data with a broad application base (19) and is capable of modeling soil loss estimates by using spatial data. Several research studies have been conducted on

GIS integration with soil loss models. Lu et al. mapped erosion severity in Rondonia, Brazilian Amazonia, by adapting GIS and remote sensing technologies with RUSLE. The soil loss model considered uniform climatic conditions and excluded rainfall erosivity and support practice factors (20). Lim et al. developed a GIS-based sediment assessment tool for erosion management, applicable for small watersheds. This study developed a GIS-based RUSLE soil loss model and included three additional modules; downstream sediment basin simulations, sediment yield calculations from a single storm event, and a GIS interface for web applications (7). Ashiagbor

et al. (21) utilized GIS tools with RUSLE to develop a soil erosion risk model for the Densu River Basin in Ghana that categorized 3% of the basin under the risk of severe erosion. Rodrigues et al. (22) presented a GIS-based soil loss model that integrated RUSLE for watershed streams in the Brazilian Cerrado, including rural areas with changing vegetation cover and land use.

Another study on the GIS-based RUSLE model was conducted in northwest Ethiopia by integrating remote sensing technology and identifying areas requiring erosion control in the Dembecha District (23). Lanorte et al. (24) used a similar approach for post-fire soil erosion risk assessment in southern Italy. These studies focused on erosion risk in watersheds and basins, considering location-specific conditions for parameter calculations.

While developing soil loss analysis, considering the impact of sediment-sensitive watersheds on downstream waterbodies has a significant role in risk analysis. For example, in the State of California, discharges are responsible to identify sediment-sensitive watersheds through site-specific analysis or GIS guidance maps (25).

RUSLE has been applied in mining, construction, and reclamation projects (26), yet there is little research in

relation to soil loss models for construction site applications. Literature in relation to RUSLE in construction erosion includes a study by Yoon et al. (27) that estimated the soil erosion rate of construction sites in coastal catchments using RUSLE. Moreover, Trenouth and Gharabaghi (12) developed event-based soil loss models of three different construction sites by using multiple linear regression and artificial neural networks on USLE. These studies presented the applicability of soil loss models on construction sites but did not integrate visual GIS models. The use of a GIS-based RUSLE model has the potential to significantly enhance SWPPPs during construction planning by guiding designers in identifying critical areas prone to higher rates of soil loss. This study advances the use of RUSLE presented in previous studies by introducing an innovative approach that creates a visual soil loss model on a national scale that is suitable for most construction scenarios in CONUS.

Methodology

Data for each corresponding parameter in RUSLE were prepared in individual layers to develop the GIS model in this study. ArcMap[®] 10.7.1 GIS software was used to model soil loss in tonnes per Ha per year (tons/acre/year) as a map layer using RUSLE calculations to calculate the amount considering the five input parameters (R, K, LS, C, and P: see Equation 1, above). R and K factor layers were created for CONUS. Three unique construction scenarios were analyzed for calculating the LS-factor from commercial, residential, and highway site plans. C and P factors were set as constant values, considering “typical” cover and practice parameters on construction sites. Further detail on the calculation of each factor and resulting RUSLE layer production is included in the following sections.

Rainfall-Runoff Erosivity (R) Factor

The RUSLE R factor provides a measure of rainfall-runoff erosivity by considering the annual summation of storm erosivity values, dependent on the total storm energy and storm intensity (13). R factor data were visualized by digitizing four isoerodent maps that were created by Wischmeier and Smith in 1978: (i) Eastern U.S., (ii) Western U.S., (iii) California, and (iv) Oregon and Washington (13, 28). Isoerodent maps display R factor values for CONUS using contour lines that pass through equal rainfall erosivity values (14). These maps were developed by using historical rainfall intensity-duration-frequency (IDF) data by considering kinetic energy contained within the storm and the intensity of the storm events. R factor values were updated by researchers in further studies based on the two-year frequency and 6 h

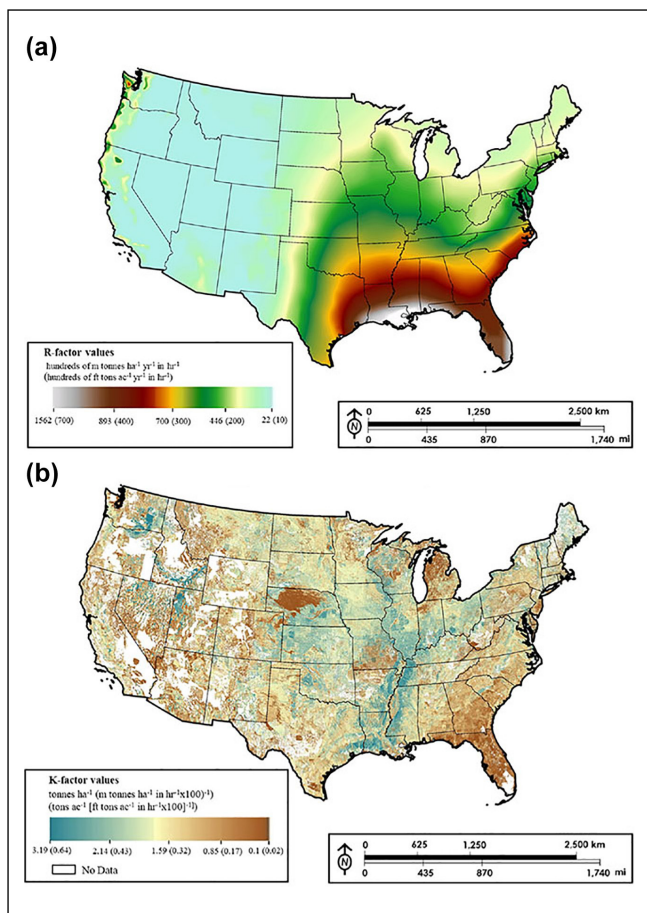


Figure 1. Rainfall erosivity (R factor) and soil erodibility (K factor) maps for CONUS: (a) rainfall-runoff erosivity and (b) soil erodibility.

rainfall duration (29). The processed R factor layer in this study consists of historical data; however, rainfall data show changes over time because of climate change. Thus, it is important to note that the model may require updating in the future in response to the non-stationary characteristic of the rainfall data. The four existing isoerodent maps were digitized in ArcMap[®] to develop .shp files, which effectively converted hardcopy or printed maps into a raster format to display data as a composition of pixels graphically. The R factor data ranged between 22 and 1,569 meter tonnes $\text{Ha}^{21} \text{ year}^{21}$ in hr^{21} 3 100 (10 and 700 [ft tons acre²¹ year²¹ in hr²¹] 3 100). The digitizing process required conversion of the existing projection from Albers Area Equal Iconic projection to Albers projection with a North American Datum of 1983.

The projected isoerodent maps were imported into an AutoCAD[®] file (13) to stitch them together to process a complete isoerodent map of CONUS. Isoerodent contour lines were digitized using the spline command in

AutoCAD[®], which creates a smooth, non-uniform curve passing through defined control vertices. The curves were extended beyond their existing boundaries to increase the interpolation accuracy between the lines when analyzed in GIS. A .dxf file of the U.S. boundaries was imported into the AutoCAD[®] file and orthorectified to the R factor contours. The .dxf file was saved and imported into ArcMap[®] using ArcCatalog[®]. The imported .dxf file was converted into a .shp file in polyline format. The attribute table of the digitized isoerodent map was then prepared by manually assigning R factor values for each contour line and using the “contour to raster” tool in ArcMap[®] to achieve the polyline format. This tool created the final layer using nearest-neighbor interpolation and resulted in the R factor layer for CONUS, as shown in Figure 1a. The figure displays R factors between 22 and 1,569 tonnes $\text{Ha}^{21} \text{ year}^{21}$ in hr^{21} 3 100 (10 and 700 [ft tons acre²¹ year²¹ in hr²¹] 3 100). Light blue-colored sections present low R factor values, and white-colored sections represent high rainfall erosivity factor values.

From the map displayed in Figure 1a, it can be observed that southeastern states have the highest R factor values among CONUS. It can be observed from the digitized R factor map that Florida, Louisiana, and the coastal counties of Alabama and Georgia have the highest rainfall erosivity values, approximately 1,562 hundreds of m tonnes $\text{Ha}^{21} \text{ year}^{21}$ in hr^{21} (700 hundreds of ft tons acre²¹ year²¹ in hr²¹). Among major cities, Houston, Jacksonville, Atlanta, and Seattle have the highest R factor. The majority of the west coast of CONUS has the lowest R factor values.

Soil Erodibility (K) Factor

The K factor represents the impact of soil properties on soil loss, and it is estimated based on natural runoff and rainfall simulation plots (14). K factor changes depending on the soil texture class, organic matter content, and hydraulic conductivity. Typically, U.S. soils have K factor values ranging between 0.02 to 0.64 (30). Soils with high clay content have low K factor values, indicative of their resistance to detachment. Silty soils, which are more prone to detachment and have high soil loss rates, have the highest K factor values (29). The U.S. Department of Agriculture (USDA) Soil Survey Geographic Database (SSURGO) contains data for soil properties in tabular or map format based on the data from the National Cooperative Soil Survey (30). This database was developed by the National Resources Conservation Service to provide digitized soil data for planning purposes (30). This database includes information on soil erosion factors in tabular format and provides the necessary information to create a nationwide K factor map. The K factor information for the whole soil survey area was

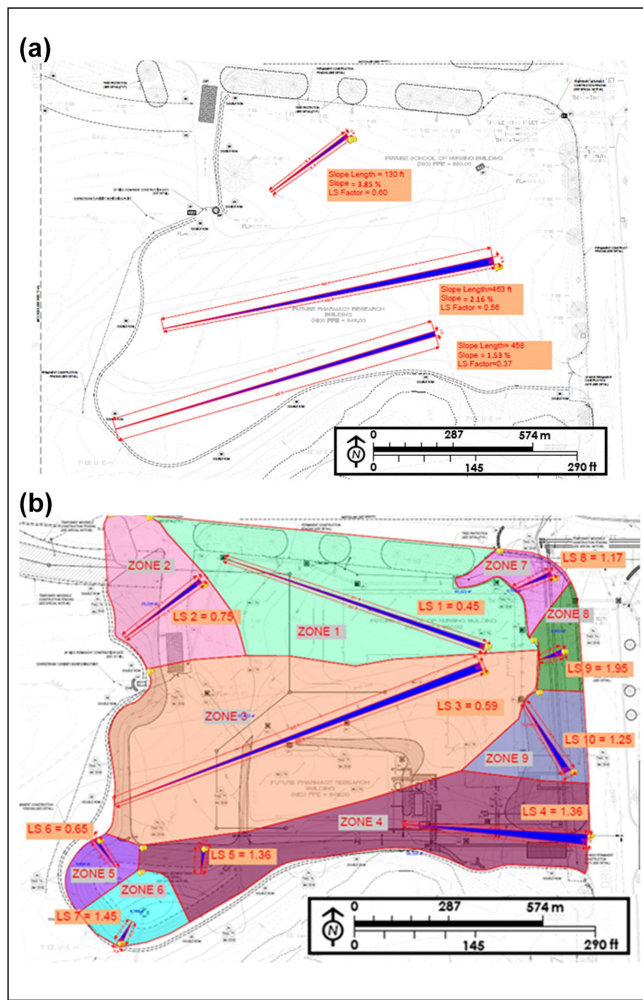


Figure 2. Length-of-slope (LS-factor) calculation for individual slopes in Bluebeam Revu[®]: (a) slope percent and slope-length measurements and (b) assigning LS factors for each zone area.

identified from the “chorizon” table, which provides soil information for the C soil horizon. C horizon soil data were selected for this study since this horizon represents the unconsolidated parent material and because topsoil horizons are typically removed early in the land-grading process of construction. Displaying this data on a map unit raster required the aggregation of “chorizon” table data to the map unit level, representing each feature class on a map to a corresponding numerical code. Data aggregation was applied in ArcMap[®] using the join tool on “component” and “chorizon” tables based on the component key field. The “component” table included the map unit key field required for assigning geolocations to each data point.

The resulting table was joined with the map unit raster; the lookup tool was used to process the raster where K factor values were stored in the “VALUE” field. Figure 1b displays the developed K factor map. According to the K factor map, soil erodibility factor

values range between 0.02 and 0.64. Blue-toned data points represent high erodibility, while brown-toned data points highlight locations with low erodibility. Based on the digitized K factor layer, the highest values can be seen in Mississippi, Louisiana, Kansas, and Illinois, while the lowest values can be observed in Nebraska, Florida, and Georgia. Several cells, primarily in pockets across states in the western U.S.A., did not have data within the SSURGO database. Missing data were visualized as white cells on the K factor raster.

Length-of-Slope (LS) Factor

LS factor is used to determine the erosivity of topography by accounting for the inclination and length of a slope. The equation to determine LS was developed for agricultural purposes with the use of U.S. customary units in Wischmeier’s study (13), as shown in Equation 2:

$$LS = (l=72:6)^m (65:41 \sin^2 u + 4:56 \sin u + 0:065) \delta 2P$$

where

LS = LS factor

l = slope length (ft)

u = slope angle

m = slope-length exponent

0.5 if slope .5%

0.4 if 3.5% \ slope \ 4.5%

0.3 if 1% \ slope \ 3%

0.2 if slope \ 1%

Larger LS values indicate a higher degree of erosivity from the slope. Typically, LS values range between 0.05 to 72.15 on freshly prepared construction sites (14). While an LS map could have been created for the entire U.S. using existing digital elevation data, construction activities often include grading operations that alter existing topographic conditions. Thus, three types of construction sites were analyzed to determine representative LS factors for (i) residential, (ii) commercial, and (iii) highway developments. These three construction site categories were used to develop composite LS factors representative of soil loss risk regardless of the location of a project within CONUS. A representative construction project was selected for each construction scenario category to estimate soil loss risks in CONUS.

Residential and commercial construction LS factors were calculated from project sites located in Alabama. Slopes on site were identified from post-construction topographic maps. The projects included several slopes, each examined for individual LS-factor calculations. The slope length and slope percent of these individual slopes were determined in Bluebeam Revu[®] software, as shown in Figure 2a. Areas governed by a given slope were assigned a zone number for weighted area calculations

Table 1. Length-of-Slope (LS) Factor for Different Construction Scenarios

Construction type	Number of assessed slopes	Total area (acres)	Weighted LS factor
Residential	19	25.4	1.54
Commercial	10	6.2	0.82
Highway	12	8.9	1.51

based on the topography. Figure 2b illustrates the calculated values of LS factors for each assigned zone on the commercial construction site plan in the Bluebeam Revu® software.

LS factors were identified using the LS table for construction sites provided by Renard et al. (14). This table presents LS factor values for the high ratio of rill to interrill erosion that can be seen in highly disturbed soil conditions. Areas that contributed to each slope were calculated, and weighted factors were computed for each zone by considering the total area. The weighted averages of LS factors were calculated based on the area of slopes by multiplying weighted area factors with LS factor values for individual slopes and adding these values to estimate the LS factor value for the total area. In total, 37 values were weighted, and the average of these values provided a representative LS factor value for each site. Based on this calculation, the weighted average for residential construction was 1.54. This methodology was repeated for a commercial construction project located in Alabama, which had a weighted average of LS factors of 0.82.

For highway construction, LS factor was computed on a 1.6 km (1 mi) section of highway construction on the U.S. 30 site in Tama County, Iowa. The project entailed the construction of a four-lane-divided highway section. A digital surface model (DSM) was created by applying photogrammetry techniques on aerial imagery captured by unmanned aerial system (31, 32). This DSM was used as an input raster layer for the contour tool in ArcMap® and a feature class of contours was created from this raster surface. The assessment to identify the weighted average of LS area, repeated from the other construction scenarios, was applied and determined to be 1.51. Table 1 summarizes LS factors for the three construction sites.

Cover Management (C) and Support Practice (P) Factors

The C factor is the most critical factor for RUSLE calculations since soil loss is proportional to exposed soil. Soil cover reduces the erosive impact of rainfall, reduces runoff velocities, and promotes infiltration. Cover management factor values range from 0 to 1, where mechanically prepared sites with no live vegetation have a cover management factor value of approximately 1. C factor values

on slopes protected with straw, hay, crushed stone, or wood chips may show a decrease down to 0.02 (13). The P factor is typically identified based on tillage and crop rotation practices for agricultural purposes; however, on construction sites, this factor describes the efficiency of the sediment control practices, including silt fences, sediment basins, sediment barriers, and traps. Changing site conditions make the P factor less reliable; thus, this factor is usually considered to be 1 during construction (13, 26, 33).

In this study, soil loss analyses were primarily conducted for construction conditions that consisted of overturned earth and exposed soils. Thus, no cover management practices were considered, yielding a C factor value of 1 for all scenarios included in this study (13). Similarly, exposed soils yielded a P factor value of 1 (33). In addition, a layer that considers a significant decrease in C and P factors was prepared for evaluating the impact of E&SC practices on soil loss.

Soil Loss Calculation

RUSLE soil loss maps for CONUS were prepared after completing each parameter layer. Soil loss maps were processed using the *raster calculator* tool to visualize soil loss for the three different construction type scenarios anywhere in CONUS. Each RUSLE parameter was a value field, and the raster calculator multiplied following the RUSLE equation. An additional map was processed to evaluate estimated average soil loss amounts for each state using the *zonal statistics tool* in ArcMap®. Moreover, a customizable soil loss map was prepared considering the product of only the R, K, C, and P factors; the LS factor was omitted. This map allows designers to select a site-specific LS factor for the soil loss model if desired.

Results and Discussion

The soil loss calculation for CONUS provides a significant dataset for enhancing design procedures in construction stormwater management. This study showed that individual soil loss factors could be computed as separate layers using GIS tools by combining various computation methods and serving as inputs to create a soil loss model for CONUS by considering different construction

Table 2. Soil Loss Risk Classes

Soil loss risk classes	Soil loss (tonnes/Ha/year)	Soil loss (tons/acre/year)	Priority rank
Very low risk	0–11	0–5	10
Low risk	11–22	5–10	9
Moderate risk	22–45	10–20	8
High risk	45–67	20–30	7
Very high risk	67–111	30–50	6
Very high risk*	111–201	50–90	5
Very high risk**	201–379	90–170	4
Very high risk***	379–736	170–330	3
Very high risk****	736–1450	330–650	2
Very high risk*****	1450+	650+	1

Note: *, **, ***, ****, *****subcategory of very high soil loss risk class.

scenarios. Rainfall erosivity and soil erodibility maps were produced as a part of this study by combining existing datasets in the literature. The results showed that displaying these layers as a complete dataset in one single map provides a user-friendly data representation that would reduce complicated tables and printed maps.

As a result of this study, soil loss values for CONUS were calculated using the RUSLE equation with the inputs of soil loss factor layers created in ArcMap®. Haregeweyn et al. (34) and Zerihun et al. (23) described soil loss from analyzed basin sites in Ethiopia and provided a classification with five categories in units of tonnes per Ha per year [tons/acre/year]: very low (0–11 [0–5]), low (11–22 [5–10]), moderate (22–45 [10–20]), high (45–90 [20–40]), and very high (-90 [-40]). Calculated soil losses in this study exceeded 90 tonnes per Ha per year (40 tons/acre/year); thus, six additional categories were added, as shown in Table 2. This categorization provided an efficient way to identify areas prone to soil loss in CONUS, which would guide designers to prioritize vulnerable areas on construction sites. However, an LS map could have been created for the entire U.S.A. using existing elevation data. Moreover, priority ranking numbers were assigned to soil loss risk classes in to emphasize areas requiring significant precautions (Table 2).

Three output maps were produced to visualize annual soil loss amounts for three construction scenarios (residential, commercial, and highway) in CONUS. The resulting map layers of soil loss models for residential, commercial, and highway construction scenarios are illustrated in Figure 3. Cells displayed in white lack soil loss calculations because of missing K factor information. The results indicate that maximum soil loss amounts on residential, commercial, and highway construction scenarios were 1,464, 706, and 1,302 tonnes per Ha per year (653, 315, and 581 tons/acre/year), respectively. The residential construction site scenario showed the highest soil

loss of the three scenarios, potentially in part to its highest weighted average of LS factor.

Figure 3a displays the soil loss map for residential and highway construction sites in CONUS. The most vulnerable areas on the map are Louisiana, western Texas, eastern Alabama, Mississippi, Arkansas, and western Tennessee. The highway construction case showed similar results to the residential construction scenario. The similarity in map results is explained by the similar weighted average of the LS factors calculated for both the residential and highway cases (1.54 and 1.51, respectively). According to the processed soil loss map, it can be observed that if a particular residential construction site were located in the southeastern U.S.A., it would be prone to very high soil loss risk. Conversely, if the same project were located in the Midwest, it would be primarily subjected to moderate soil loss risk and somewhat very high and high soil loss risk. In the western U.S.A., the soil loss risk displayed was low and very low, except along the coast. A residential project would be susceptible to moderate and high soil loss rates in Washington, Oregon, and California.

Figure 3b shows the soil loss map for the commercial construction scenario. Results from the commercial construction soil loss map, shown in Figure 3b, indicate that commercial construction would not leave land susceptible to very high soil loss rates if located anywhere in CONUS. Exceptions include the southeastern states, including Louisiana, western Texas, Mississippi, Arkansas, and western Tennessee. The Midwest, eastern U.S.A., and coastal zones of western U.S.A. showed low, moderate, and somewhat high soil loss risk. The majority of western states did not display any significant soil loss risk for commercial construction type.

Figure 3c illustrates state-wide average soil loss values for each state in the study area by considering a typical construction scenario that includes LS, C, and P factor values set at 1. This map provided the opportunity to

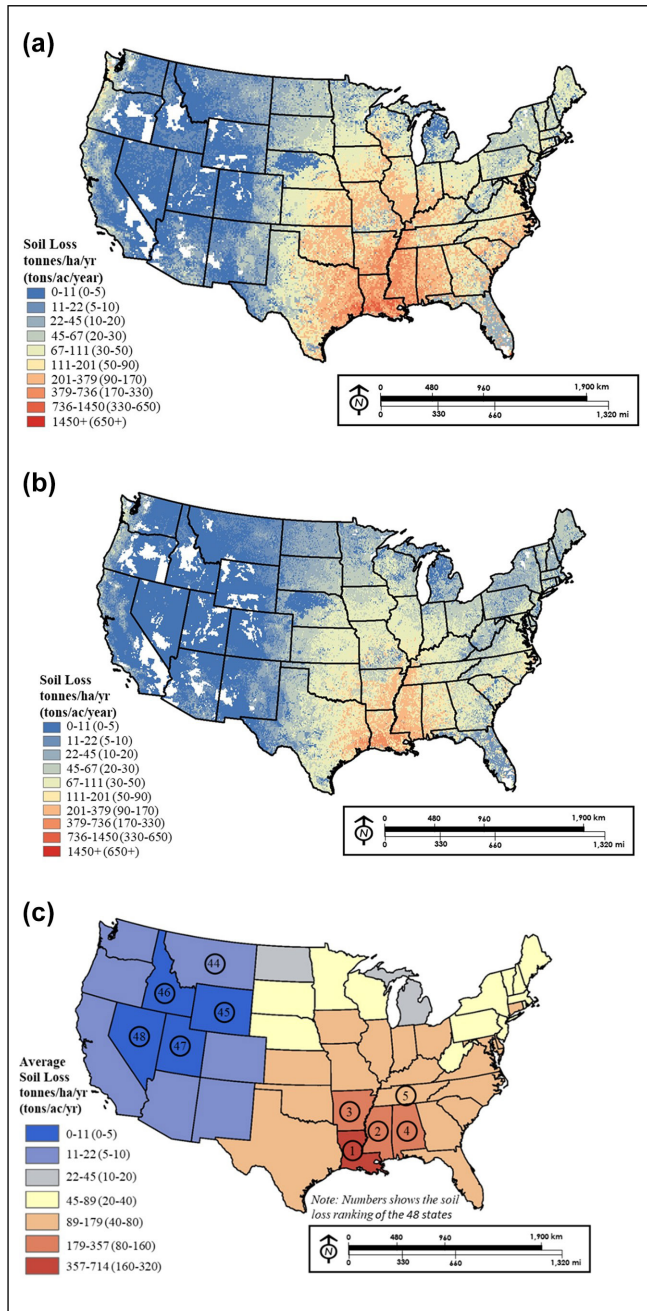


Figure 3. Soil loss maps based on construction type: (a) residential and highway construction soil loss map, (b) commercial construction soil loss map, and (c) customizable state average soil loss map.

rank the 48 states by soil loss risk severity. Zonal statistics for state-specific average soil loss amounts indicated that Louisiana has the highest soil loss risk with the soil loss amount of 395 tonnes per Ha per year (177 tons/acre/year), followed by Mississippi 330 tonnes per Ha per year (148 tons/acre/year), Arkansas 223 tonnes per Ha

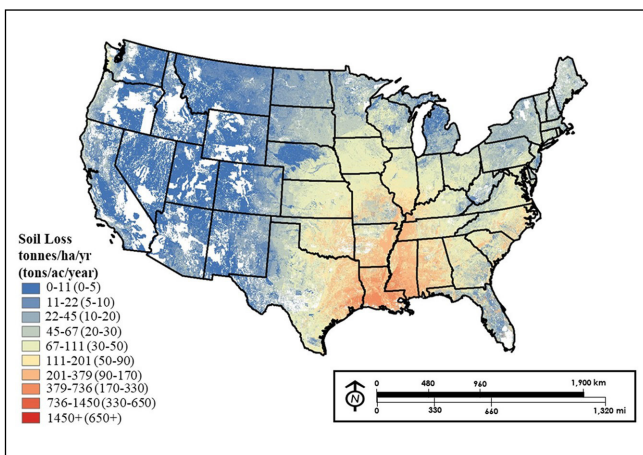


Figure 4. Customizable soil loss map for construction sites in the contiguous U.S.A.

per year (100 tons/acre/year), and Alabama 216 tonnes per Ha per year (97 tons/acre/year). These states have high R and K factor values, which increases the risk of erosion. The states with the lowest soil loss risk are Nevada, Utah, Idaho, and Wyoming because of low R and K factor impacts.

Highway and residential construction scenarios indicated greater soil loss risk because they have steeper slopes compared with commercial construction; however, this may not be applicable for all commercial construction projects in the U.S.A. Every construction project has unique topographic features, dependent on the location and grading plan, and thus poses a limitation to this study. Low soil loss risk areas do not indicate that lack of measurements would be acceptable for these locations. This tool is designed to support designers and practitioners in identifying areas that they would prioritize for implementing necessary E&SC precautions.

The aim of this study was to provide a general assessment of soil loss severity considering three different construction type scenarios. The research provided a customizable layer for designers to be adapted to typical construction scenarios. Figure 4 displays the customizable soil loss map that includes the LS factor as 1, which would allow adjustments to the map based on site-specific LS factors by multiplying the job site's LS factor value with this customizable layer.

The map's results are still displayed in tonnes per Ha per year (tons/acre/year) since the LS factor is unitless. This customizable layer also shows that the southeastern U.S.A. is more prone to soil loss than other regions. However, the results might differ depending on the site-specific LS factor input to the model. The output provides a valuable tool for designers to rapidly evaluate the soil loss risk of construction sites anywhere in the U.S.A.

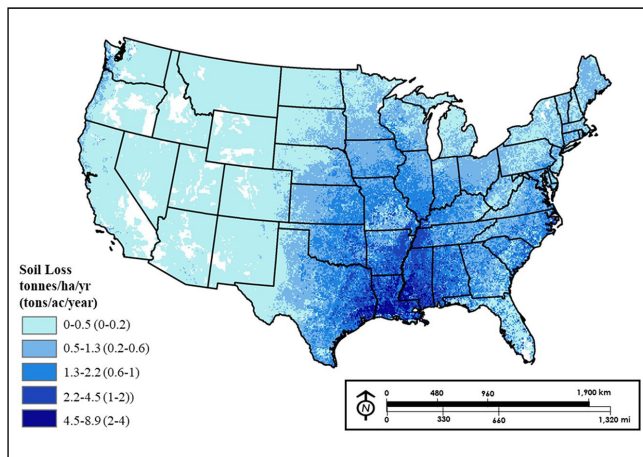


Figure 5. Soil loss map with cover management (C) and support practice (P) factor values.

using site-specific LS factor input. Site-specific LS-factors can be calculated easily using topographic plans of the sites, as discussed in the methodology section of this paper. Designers can use this tool to understand better the severity of soil loss risk based on location while preparing construction E&SC plans.

Soil loss maps in this study were mainly processed by considering cover management (C factor) and support practice (P factor) as 1, as mentioned in the methodology section; however, it is important to evaluate the change in soil loss when changing C and P factors. The study also created an additional map that considers the use of cover management and support practices on construction sites. The customizable soil loss map was used to develop the additional map by changing C and P factor values. The decrease in C and P factor values indicates the protection of slopes with E&SC practices. These factors range between 0 and 1, where 1 indicates no cover management or support practices on site. To represent a higher level of E&SC practice implementation, 0.1 was selected as an input value for map processing. Figure 5 presents the resulting soil loss layer for CONUS for reduced C and P factors.

In Figure 5, light blue tones represent the least amount of soil loss while dark blue tones show high values for soil loss. The comparison of this layer with the customizable layer shown in Figure 4 provides significant findings for evaluating the significance of E&SC practices. The results reveal a significant decrease in soil loss in high-risk areas (i.e., southeastern states and coastal parts of western states). For instance, the maximum soil loss amount for Louisiana, which has the highest erosive risk, was calculated as approximately 1,000 tonnes per Ha per year (448 tons/acre/year). However, this value drops to 9.4 tonnes per Ha per year (4.2 tons/acre/year), which

shows a 99% decrease in soil loss when implementing E&SC practices.

Conclusion

Construction site soil loss and the downstream discharge of sediment pose significant environmental implications to receiving waterbodies. The design of effective E&SC practices on construction sites is an essential component for proper SWPPP development. RUSLE can serve as a predictive model to estimate soil loss risks and identify areas of particular concern on a site. GIS-based RUSLE tools have been helpful in modeling soil loss in agricultural studies. With a similar approach, this study utilized RUSLE for soil loss risk visualization through GIS applications and provided a general soil loss risk assessment for construction activities in CONUS. This research investigated its application to construction applications in residential, commercial, and highway construction scenarios and evaluated the soil loss severity in these cases by considering the project location anywhere within CONUS. The study also provided a customizable tool for designers capable of computing annual soil loss amounts anywhere in CONUS for a site-specific LS factor.

This study aimed to support construction stormwater designers during SWPPP preparation by providing an innovative tool capable of displaying vulnerable areas requiring precaution on sites. Soil loss maps of CONUS for construction sites were prepared using GIS tools and RUSLE. However, site-specific topographic characteristics created a limitation for processing a single map that would be valid regardless of construction type; therefore, three different construction scenarios were assessed with varying LS factors. The sample size used in LS factor calculation for construction scenarios was not large enough to provide a broad estimation, which created a limitation for identifying representative LS factor values in the study. The assessment results indicated that southeastern states tend to have high soil loss risk for residential, commercial, and highway construction sites with soil loss amount up to 1,464, 706, and 1,302 tonnes per Ha per year (653, 315, and 581 tons/acre/year), respectively.

Moreover, the LS factor limitation resulted in a customizable map, allowing designers to work with site-specific LS factors while utilizing this tool. This customizable map has also benefitted this study for evaluating the impact of the use of E&SC practices by analyzing the soil loss with changing practice factors. An additional map was produced based on the customizable soil loss map by reducing C- and P factors. The results indicated a 99% reduction in soil loss when E&SC is maintained on potential construction sites.

Another limitation of the developed model was data reliability over time for R and K factor maps. The processed R and K factor maps included historical data that may potentially change over time based on the non-stationary nature of rainfall events and changing soil characteristics throughout different construction phases. The historical data obtained from national databases may not provide precise results for soil loss evaluation of smaller areas; however, it would provide a general overview on identifying risk areas. For increased accuracy in evaluations, data presented in this study may require site-specific updates in response to changing soil and rainfall characteristics over time to maintain data fidelity.

The results of this study provide an innovative soil loss model for future research studies and potentially for practical application. Future studies may improve this study's results by completing missing data in K factor information from additional sources and extending the sample size for LS factor calculation by evaluating more construction projects and plans. Moreover, the assessment of additional construction types with this tool would improve the results of this study. With appropriate modifications through future research efforts, the presented tool would potentially extend its usage in different applications outside of construction activities, such as assessments on wildfire post-burn watersheds and land management activities. The current version of the developed tool could be utilized for education in SWPPP development by displaying the impact of changing factors on soil loss. The presented soil loss model has the capability of guiding practitioners for Best Management Practice (BMP) implementation in different phases of the construction. In addition, the soil loss results of this study may be clipped into a smaller spatial scale and provide a general soil loss risk assessment for designers while developing SWPPP. However, site-specific data updates on the presented tool would be necessary for small-scale soil loss risk analysis. The study proves the compatibility of GIS with RUSLE and guides designers with macro-scale data to improve SWPPP development. The developed tool will be available after completion of fine-tuning of the model and development of a user-friendly interface.

Author Contributions

The authors confirm contribution to the paper as follows: study conception and design: M. A. Perez, B. Kazaz; data collection: B. Kazaz, L. C. Dickey; analysis and interpretation of results: B. Kazaz, M. A. Perez; draft manuscript preparation: B. Kazaz, J. C. Schussler, M. A. Perez. All authors reviewed the results and approved the final version of the manuscript.

Declaration of Conflicting Interests

The author(s) declared no potential conflicts of interest with respect to the research, authorship, and/or publication of this article.

Funding

The author(s) received no financial support for the research, authorship, and/or publication of this article.

ORCID iDs

Billur Kazaz  <https://orcid.org/0000-0001-9292-0928>
Jaime C. Schussler  <https://orcid.org/0000-0001-8568-3338>
LouLou C. Dickey  <https://orcid.org/0000-0003-4228-1640>
Michael A. Perez  <https://orcid.org/0000-0001-5156-9369>

Data Accessibility Statement

Some or all data, models, or codes that support the findings of this study are available from the corresponding author on reasonable request. The following data sets are available: raw measurements collected during experimentation and photographs documenting experiments.

References

1. U.S. Congress. Federal Water Pollution Control Act. 33 U.S.C. 1251 et seq., U.S. Congress, 2002, p. 234.
2. U.S. Environmental Protection Agency. *Construction General Permit (CGP)*. Environmental Protection Agency, Washington, D.C., 2017.
3. U.S. Environmental Protection Agency. *Developing Your Stormwater Pollution Prevention Plan: A Guide for Construction Sites*. Environmental Protection Agency, Washington, D.C., 2007.
4. Perez, M. A., W. C. Zech, W. N. Donald, and X. Fang. Design Methodology for the Selection of Temporary Erosion and Sediment Control Practices Based on Regional Hydrological Conditions. *Journal of Hydrologic Engineering*, Vol. 21, No. 4, 2016, P. 05016001. [https://doi.org/10.1061/\(asce\)he.1943-5584.0001328](https://doi.org/10.1061/(asce)he.1943-5584.0001328).
5. Whitman, J. B., W. C. Zech, W. N. Donald, and J. J. LaMondia. Full-Scale Performance Evaluations of Various Wire-Backed Nonwoven Silt Fence Installation Configurations. *Transportation Research Record: Journal of Transportation Research Board*, 2018. 2672: 68–78.
6. Schussler, J. C., B. Kazaz, M. A. Perez, J. Blake Whitman, and B. Cetin. Field Evaluation of Wattle and Silt Fence Ditch Checks. *Transportation Research Record: Journal of the Transportation Research Board*, 2021. 2675: 281–293.
7. Lim, K. J., M. Sagong, B. A. Engel, Z. Tang, J. Choi, and K. S. Kim. GIS-Based Sediment Assessment Tool. *Catena*, Vol. 64, 2005, pp. 61–80. <https://doi.org/10.1016/j.catena.2005.06.013>.
8. Ganapati, B. P., and H. Ramesh. Assessment of Soil Erosion by RUSLE Model Using Remote Sensing and GIS – A Case Study of Nethravathi Basin. *Geoscience Frontiers*, Vol. 7, No. 6, 2016, pp. 953–961. <https://doi.org/10.1016/j.gsf.2015.10.007>.
9. Renard, K. G., D. C. Yoder, D. T. Lightle, and S. M. Dabney. Universal Soil Loss Equation and Revised Universal Soil Loss Equation. In *Handbook of Erosion Modelling* (Morgan, R. P. C., and M. A. Nearing, eds.), Blackwell Publishing, Hoboken, NJ, 2011, pp. 135–167.

10. Parveen, R., and U. Kumar. Integrated Approach of Universal Soil Loss Equation (USLE) and Geographical Information System (GIS) for Soil Loss Risk Assessment in Upper South Koel Basin, Jharkhand. *Journal of Geographic Information Systems*, Vol. 4, No. 2, 2012. <https://doi.org/10.4236/jgis.2012.46061>.
11. Dissmeyer, G. E., and G. R. Foster. A Guide for Predicting Sheet and Rill Erosion on Forest Land. Technical Publication SA-TP 11. U.S. Department of Agriculture, Forest Service, Atlanta, GA, 1981.
12. Trenouth, W. R., and B. Gharabaghi. Event-Based Soil Loss Models for Construction Sites. *Journal of Hydrology*, Vol. 524, 2015, pp. 780–788. <https://doi.org/10.1016/j.jhydrol.2015.03.010>.
13. Wischmeier, W. H., and D. D. Smith. *Predicting Rainfall Erosion Losses—A Guide to Conservation Planning*. Agriculture Handbook No. 537. U.S. Department of Agriculture, Beltsville, MD, 1978.
14. Renard, K. G., G. R. Foster, G. A. Weesies, D. K. McCool, and D. C. Yoder. *Predicting Soil Erosion by Water: A Guide to Conservation Planning with the Revised Universal Soil Loss Equation (RUSLE)*. U.S. Department of Agriculture, Washington, D.C., 1997.
15. Williams, J. R. Sediment Routing for Agricultural Watersheds. *JAWRA Journal of the American Water Resources Association*, Vol. 11, No. 5, 1975, pp. 965–974. <https://doi.org/10.1111/j.1752-1688.1975.tb01817.x>.
16. Alewell, C., P. Borrelli, K. Meusburger, and P. Panagos. Using the USLE: Chances, Challenges, and Limitations of Soil Erosion Modelling. *International Soil and Water Conservation Research*, Vol. 7, No. 3, 2019, pp. 203–225. <https://doi.org/10.1016/j.iswcr.2019.05.004>.
17. Risse, L. M., M. A. Nearing, A. D. Nicks, and J. M. Laflen. Error Assessment in the Universal Soil Loss Equation. *Soil Science Society of America*, Vol. 57, 1993. <https://doi.org/10.2136/sssaj1993.03615995005700030032x>.
18. Millward, A. A., and J. E. Mersey. Adapting the RUSLE to Model Soil Erosion Potential in a Mountainous Tropical Watershed. *Catena*, Vol. 38, No. 2, 1999, pp. 109–129. [https://doi.org/10.1016/S0341-8162\(99\)00067-3](https://doi.org/10.1016/S0341-8162(99)00067-3).
19. Maguire, D. J. An Overview and Definition of GIS. *Geographical Information Systems: Principles, Techniques, Management and Applications* (Longley, P. A., M. F. Goodchild, D. J. Maguire, and D. W. Rhind eds.), John Wiley and Sons, Newyork, NY, 1991, pp. 9–20. <http://www.wiley.com/legacy/wileychi/gis/volumes.html>.
20. Lu, D., G. Li, G. S. Valladares, and M. Batistella. Mapping Soil Erosion Risk in Rondonia, Brazilian Amazonia: Using RUSLE, Remote Sensing and GIS. *Land Degradation and Development*, Vol. 15, No. 5, 2004, pp. 499–512. <https://doi.org/10.1002/lde.634>.
21. Ashiagbor, G., E. K. Forkuo, P. Laari, and R. Aabeyir. Modeling Soil Erosion Using RUSLE and GIS Tools. *International Journal of Remote Sensing & Geoscience (IJRSG)*, Vol. 2, 2012, pp. 7–17.
22. Rodrigues, E., V. M. Bacani, and E. Panachuki. Modeling Soil Erosion Using RUSLE and GIS in a Watershed Occupied by Rural Settlement in the Brazilian Cerrado. *Natural Hazards*, Vol. 85, No. 2, 2017, pp. 851–868. <https://doi.org/10.1007/s11069-016-2607-3>.
23. Zerihun, M., M. S. Mohammedyasin, D. Sewnet, A. A. Adem, and M. Lakew. Assessment of Soil Erosion Using RUSLE, GIS, and Remote Sensing in NW Ethiopia. *Geoderma Regional*, Vol. 12, 2018, pp. 83–90. <https://doi.org/10.1016/j.geodrs.2018.01.002>.
24. Lanorte, A., G. Cillis, G. Calamita, G. Nole', A. Pilogallo, B. Tucci, and F. De Santis. Integrated Approach of RUSLE, GIS, and ESA Sentinel-2 Satellite Data for Post-Fire Soil Erosion Assessment in Basilicata Region (Southern Italy). *Geomatics, Natural Hazards, and Risk*, Vol. 10, No. 1, 2019, pp. 1563–1595. <https://doi.org/10.1080/19475705.2019.1578271>.
25. State Water Resources Control Board. *Construction General Permit*. Division of Water Quality, Sacramento, CA, 2009.
26. Toy, T. J., G. R. Foster, and K. G. Renard. RUSLE for Mining, Construction, and Reclamation Lands. *Journal of Soil and Water Conservation*, Vol. 54, 1999, pp. 462–467.
27. Yoon, K. S., C.W. Kim, and H. Woo. Application of RUSLE for Erosion Estimation of Construction Sites in Coastal Catchments. *Journal of Coastal Research*, Vol. 56, 2009, pp. 1696–1700.
28. U.S. Environmental Protection Agency. *Stormwater Phase II Final Rule: Construction of Rainfall Erosivity Waiver*. No. EPA 833-F-00-014. U.S. Environmental Protection Agency, Washington, D.C., 2012, p. 12.
29. U.S. Department of Agriculture. *SSURGO Data Packaging and Use*. U.S. Department of Agriculture, Washington, D.C., November, 2012.
30. Renard, K. G., G. R. Foster, G. A. Weesies, and J. P. Porter. RUSLE: Revised Universal Soil Loss Equation. *Journal of Soil & Water Conservation*, Vol. 46, No. 1, 1991, pp. 30–33.
31. Perez, M. A., W. C. Zech, and W. N. Donald. Using Unmanned Aerial Vehicles to Conduct Site Inspections of Erosion and Sediment Control Practices and Track Project Progression. *Transportation Research Record: Journal of the Transportation Research Board*, 2015. 2528, pp. 38–48.
32. Kazaz, B., S. Poddar, S. Arabi, M. A. Perez, A. Sharma, and J. Blake Whitman. Deep Learning-Based Object Detection for Unmanned Aerial Systems (UASs)-Based Inspections of Construction Stormwater Practices. *Sensors*, Vol. 21, No. 8, 2021, p. 2834. <https://doi.org/10.3390/s21082834>.
33. Fifield, J. S. *Designing and Reviewing Effective Sediment and Erosion Control Plans*. Forester Press, Santa Barbara, CA, 2011.
34. Haregeweyn, N., A. Tsunekawa, J. Poesen, M. Tsubo, D. T. Meshesha, A. A. Fenta, J. Nyssen, and E. Adgo. Comprehensive Assessment of Soil Erosion Risk for Better Land Use Planning in River Basins: Case Study of the Upper Blue Nile River. *Science of the Total Environment*, Vol. 574, 2017, pp. 95–108. <https://doi.org/10.1016/j.scitotenv.2016.09.019>.